Crystal Structure of Rabbit Cytosolic Serine Hydroxymethyltransferase at 2.8 Å Resolution: Mechanistic Implications[†,‡]

J. N. Scarsdale, G. Kazanina, S. Radaev,[§] V. Schirch, and H. T. Wright*

Institute of Structural Biology and Drug Discovery, Virginia Commonwealth University, 800 East Leigh Street, Richmond, Virginia 23219

Received February 22, 1999; Revised Manuscript Received April 26, 1999

ABSTRACT: Serine hydroxymethyltransferase (SHMT) catalyzes the reversible cleavage of serine to form glycine and single carbon groups that are essential for many biosynthetic pathways. SHMT requires both pyridoxal phosphate (PLP) and tetrahydropteroylpolyglutamate ($H_4PteGlu_n$) as cofactors, the latter as a carrier of the single carbon group. We describe here the crystal structure at 2.8 Å resolution of rabbit cytosolic SHMT (rcSHMT) in two forms: one with the PLP covalently bound as an aldimine to the Nϵ-amino group of the active site lysine and the other with the aldimine reduced to a secondary amine. The rcSHMT structure closely resembles the structure of human SHMT, confirming its similarity to the α-class of PLP enzymes. The structures reported here further permit identification of changes in the PLP group that accompany formation of the *geminal* diamine complex, the first intermediate in the reaction pathway. On the basis of the current mechanism derived from solution studies and the properties of site mutants, we are able to model the binding of both the serine substrate and the $H_4PteGlu_n$ cofactor. This model explains the properties of several site mutants of SHMT and offers testable hypotheses for a more detailed mechanism of this enzyme.

Serine hydroxymethyltransferase (SHMT,[1] EC 2.1.2.1) is a pyridoxal 5′-phosphate (PLP) enzyme that catalyzes the reversible interconversion of serine and glycine using the coenzyme $H_4PteGlu_n$ as the one-carbon carrier. This enzyme is ubiquitous in nature because of its essential function as a major donor of one-carbon groups, via CH_2-$H_4PteGlu_n$, which are required for purine, thymidylate, and methionine biosynthesis and many other methylation reactions. In eukaryotic cells, both cytosolic and mitochondrial isoenzymes are expressed from nuclear genes (*1*) and amino acid sequences inferred from cDNA sequences are available for 32 SHMTs (*2*). All SHMTs studied to date are either homodimers or homotetramers with monomer molecular masses in the 45−54 kDa range. The extensive similarity of the central amino acid sequence among these different SHMTs indicates that they are closely related in structure and catalytic mechanism.

In addition to requiring the coenzyme $H_4PteGlu_n$, SHMT also contains PLP tightly bound to the ϵ-amino group of a Lys residue as an aldimine (termed the internal aldimine and shown as structure I in Scheme 1). Like other PLP enzymes, the substrate serine forms an external aldimine with the PLP (IV, Scheme 1) via *geminal* diamine intermediates (II and III, Scheme 1). The currently accepted mechanism for SHMT is a retroaldol cleavage of this serine aldimine to form formaldehyde and a resonance-stabilized quinonoid intermediate that absorbs near 500 nm (V, Scheme 1). Addition of a proton to the α-carbon of the amino acid in this quinonoid intermediate forms the external aldimine of glycine (IV, Scheme 1). The formaldehyde is transferred to H_4-$PteGlu_n$ to form CH_2-$H_4PteGlu_n$, and the glycine aldimine is converted to glycine, returning the enzyme to its original state (IV to I, Scheme 1) (*3*). SHMT catalyzes an exchange of the electrophilic H^+ and formaldehyde at the 2-*pro*-*S* position of glycine.

In addition to this physiological reaction with serine and glycine, SHMT has been shown, in the absence of $H_4PteGlu_n$, to cleave a number of 3-hydroxy amino acids to glycine and the corresponding aldehyde, in some cases at rates approaching the rate of serine cleavage (*3*). SHMT also stereospecifically decarboxylates aminomalonate at a rate that exceeds that of the physiological reaction (*4*).

Like other PLP enzymes, SHMT has been observed to slowly catalyze alternative reactions with nonsubstrate amino acids. Of these alternate reactions, those studied in the most detail are the slow transamination and racemization of D- and L-alanine (*5*). These occur because the α-protons of either D- or L-alanine can each be transferred to distinct bases on the enzyme to form a quinonoid complex. Transfer of a proton from a base to C4′ results in the formation of a ketimine intermediate common to all transamination reactions

[†] This work was supported by NIH Grants GM50209 (H.T.W.) and GM28143 (V.S.).

[‡] Coordinates have been deposited in the Protein Data Bank as entry 1CJ0.

* To whom correspondence should be addressed. Telephone: (804) 828-6139. Fax: (804) 827-3664.

[§] Present address: Department of Biochemistry and Molecular Biology, Wayne State University, School of Medicine, 540 E. Canfield Ave., Detroit, MI 483201.

[1] Abbreviations: SHMT, serine hydroxymethyltransferase; rc, rabbit cytosolic; hc, human cytosolic; AATase, aspartate aminotransferase; $H_4PteGlu_n$, tetrahydropteroylglutamate containing *n* glutamate residues; CH_2-$H_4PteGlu_n$, methylenetetrahydropteroylglutamate; KMES, potassium morpholinoethane sulfonate; PLP, pyridoxal 5′-phosphate; SIRAS, single isomorphous replacement anomalous scattering; MIRAS, multiple isomorphous replacement anomalous scattering.

10.1021/bi9904151 CCC: $18.00
Published on Web 06/10/1999

Scheme 1

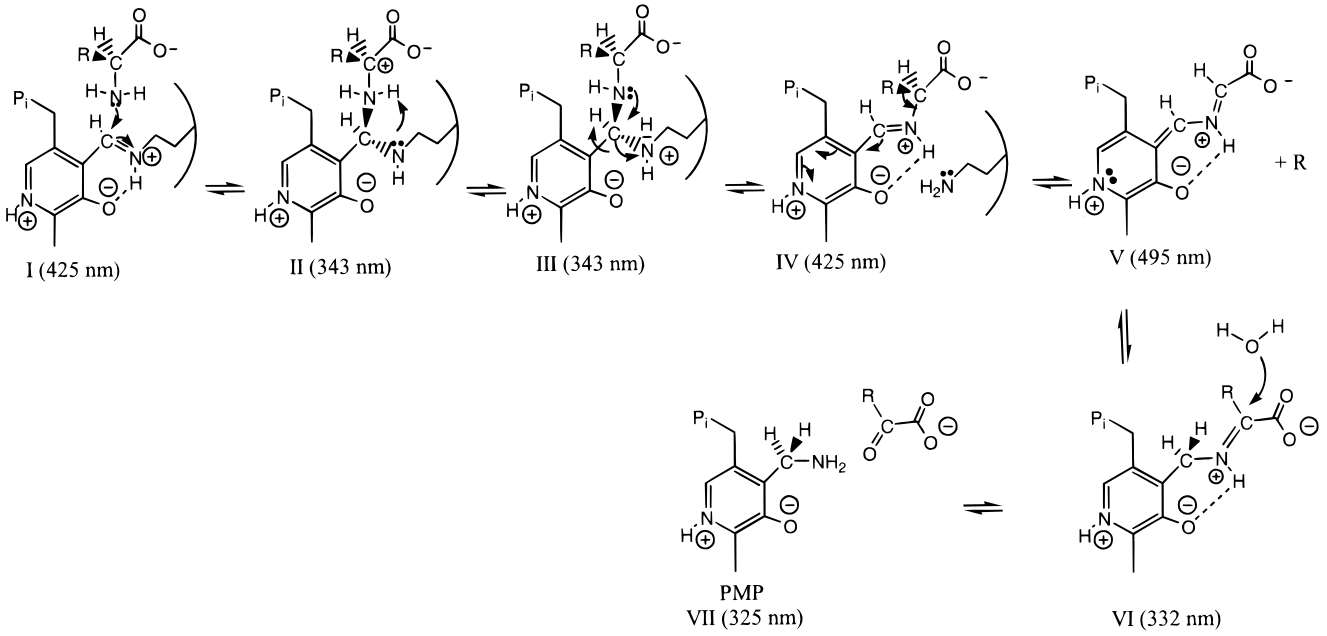

(VI, Scheme 1). Hydrolysis of this intermediate results in PMP and pyruvate (VII, Scheme 1).

Until recently, little information regarding the structure of SHMT was available. SHMT was recognized as belonging to the α-class of PLP-containing enzymes that break one of the bonds around the α-carbon of an amino acid (*6*, *7*). Many of the conserved residues in the sequences of SHMTs match conserved residues at the active site of aspartate aminotransferase (AATase), the most studied of the PLP enzymes belonging to the α-class (*8*−*10*). Subsequent studies of other members of the α-class showed that they share a conserved conformational framework, a common two-domain structure, and an active site composed of residues from two different subunits (*11*−*17*). Other members of the α-class include L-amino acid transaminases, many decarboxylases, glutamate-1-semialdehyde aminomutase, and tyrosine phenol-lyase.

Progress toward the determination of the high-resolution crystal structure of SHMT began with the crystallization of *Escherichia coli* SHMT (*11*) and was followed later by the elucidation of other crystal forms of rabbit and human enzymes (*12*, *13*). A hypothetical model for SHMT was proposed on the basis of inferred similarity to the α-class enzymes (AATase, dialkyl glycine decarboxylase, tyrosine-phenol lyase, and ornthine decarboxylase) and the results of mutagenesis experiments (*14*). Recently, the structure of human cytosolic SHMT has been published, confirming that SHMT has the same general fold as the other members of the α-group (*15*).

This study reports the crystal structure of rabbit cSHMT in two holoenzyme forms with no bound amino acid ligands: the internal aldimine in which the active site K229 forms a Schiff base linkage with the C4′ carbon of PLP and a covalent complex in which the lysine−PLP bond is reduced to a secondary amine. The structure of rcSHMT is similar to that of human cSHMT, but we are able to further infer from our structure mechanistic roles of residues at the active site, changes that occur in PLP conformation on formation of the *gem*-diamine intermediate, and a putative binding site for $H_4PteGlu_n$. The structure has also allowed us to expand the characterization of interactions which stabilize the dimer and tetramer.

EXPERIMENTAL PROCEDURES

Sequence Numbering Conventions. For consistency in comparison of results from different SHMTs, we propose a sequence numbering scheme based on alignment with the sequence of *E. coli* SHMT as a reference. Residues absent from the *E. coli* SHMT sequence but present in another SHMT ("insertions") are identified by a numerical, subscript suffix to the nearest preceding in-sequence residue number. Residues absent in an SHMT but denumerated in the *E. coli* sequence ("deletions") are skipped in sequence numbering without a change in the succeeding residues which are in correspondence with the *E. coli* sequence (Table 1). Discussion of the tight dimer of SHMT identifies an amino acid residue with a specific subunit with a prefix A or B.

Preparation and Crystallization of Enzyme. Rabbit cytosolic SHMT, mutated to alter Asn-5 to Gln, was expressed from a construct of the gene cloned into *E. coli* HMS174-(DE3) cells on a pET 22b(+) plasmid as previously described (*23*). Enzyme was isolated by rapid purification over a 2 day period. Internal aldimine-reduced SHMT was prepared by the addition of $NaCNBH_3$ to a concentration of 50 μM followed by dialysis overnight against 20 mM K_2HPO_4/KH_2PO_4, 0.2 mM EDTA, and 5 mM 2-mercaptoethanol (*19*).

Tetragonal crystals ($P4_12_12$) of reduced and unreduced rcSHMT were obtained at low ionic strength [20 mM K_2HPO_4/KH_2PO_4, 25 mM KMES or sodium Hepes (pH 7.0), 0.2 mM EDTA, and 5 mM 2-mercaptoethanol] from hanging drops initially at 3% PEG 4000 (*19*). Crystals appeared in 3−5 days and grew to maximum size in 5−7 days. Variability among crystals in the lattice order and resolution limit of diffraction was common, and it was found that freshly grown crystals were better ordered than those stored for more than 2 weeks, even in their growth medium. Heavy atom isomorphous replacements were prepared by soaking 1-week-old crystals in artificial supernatant [40 mM KMES (pH 7.0) and 0.5% PEG 4000] followed by transfer into the

Table 1: Aligned Sequences of *E. coli*, Rabbit, Human, and Sheep Cytosolic SHMTs[a]

```
          -25   -20        -10     -1 1        10          20          30          40
shmtec    ..... .......... ........MR MLKREMNIAD YDAELWQAME QEKVRQEEHI ELIASENYTS
shmtrc    .ATA. VN.G.APRDA ALWSSHEQ.. MLAQPLK..D SDAEVYDIIK KESNRQRVGL ELIASENFAS
shmthc    .MTMP VN.G.AHKDA DLWSSHDK.. MLAQPLK..D SDVEVYNIIK KESNRQRVGL ELIASENFAS
shmtsc    .MAAP VN..KAPRDA DLWSLHEK.. MLAQPLK..D NDVEVYNIIK KESNRQRVGL ELIASENFAS

                50          60          70          80                90          100
                                                                1   23    1
shmtec    PRVMQAQGSQ LTNKYAEGYP GKRYYGGCEY VDIVEQLAID RAKELFGAD.....Y A.NVQPHSGSQ
shmtrc    RAVLEALGSC LNNKYSEGYP GQRYYGGTEH IDELETLCQK RALQAYGLDP..QCW GVNVQPYSGSP
shmthc    RAVLEALGSC LNNKYSEGYP GQRYYGGTEF IDELETLCQK RALQAYKLDP..QCW GVNVQPYSGSP
shmtsc    RAVLEALGSC LNNKYSEGYP GQRYYGGTEF IDELEVLCQK RALQVYGLDP..ECW GVNVQPYSGSP

              110         120         130             140         150         160
                    1                               123    1    1          1
shmtec    ANFAVYTALL EP.GDTVLGMN LAHGGHLTHG SPVN...FSGK.LY .NIVPYGIDA.T GHIDYADLEK
shmtrc    ANFAVYTALV EPHG.RIMGLD LPDGGHLTHG FMTDKKKISATSIF FESMAYKVNPDT GYIDYDRLEE
shmthc    ANFAVYTALV EPHG.RIMGLD LPDGGHLTHG FMTDKKKISATSIF FESMPYKVNPDT GYINYDQLEE
shmtsc    ANFAVYTALV EPHG.RIMGLD LPDGGHLTHG FMTDKKKISATSIF FESMPYKVNPDT GYINYDQLEE

              170         180         190         200         210         220
shmtec    QAKEHKPKMI IGGFSAYSGV VDWAKMREIA DSIGAYLFVD MAHVAGLVAA GVYPNPVPHA
shmtrc    NARLFHPKLI IAGTSCYSRN LDYGRLRKIA DENGAYLMAD MAHISGLVVA GVVPSPFEHC
shmthc    NARLFHPKLI IAGTSCYSRN LEYARLRKIA DENGAYLMAD MAHISGLVAA GVVPSPFEHC
shmtsc    NARLFHPRLI IAGTSCYSRN LDYARLRKIA DDNGAYLMAD MAHISGLVAA GVVPSPFEHC

              230         240                 250         260         270
                                  123456789       12  1
shmtec    HVVTTTTHKT LAGPRGGLIL AKGG.........SEELYK ..KL.NSAVFPGG QGGPLMHVIA
shmtrc    HVVTTTTHKT LRGCRAGMIF YRRGVRSVDPKTGKEILYN LESLINSAVFPGL QGGPHNHAIA
shmthc    HVVTTTTHKT LRGCRAGMIF YRKGVKSVDPKTGKEILYN LESLINSAVFPGL QGGPHNHAIA
shmtsc    HVVSTTTHKT LRGCRAGMIF YRKGVRSVDPKTGKETRYN LESLINSAVFPGL QGGPHNHAIA

              280         290         300         310         320         330
shmtec    GKAVALKEAM EPEFKTYQQQ VAKNAKAMVE VFLERGYKVV SGGTDNHLFL VDLVDKNLTG
shmtrc    GVAVALKQAM TPEFKEYQRQ VVANCRALSA ALVELGYKIV TGGSDNHLIL VDLRSKGTDG
shmthc    GVAVALKQAM TLEFKVYQHQ VVANCRALSE ALTELGYKIV TGGSDNHLIL VDLRSKGTDG
shmtsc    GVAVALKQAM TPEFRAYQRQ VVANCRALAE ALMGLGYRVV TGGSDNHLIL VDLRSKGTDG

              340         350         360         370                 380         390
                                                                  12
shmtec    KEADAALGRA NITVNKNSVP NDPKSPFVTS GIRVGTPAIT RRGF..KEAEAK ELAGWMCDVL
shmtrc    GRAEKVLEAC SIACNKNTCP GD.KSALRPS GLRLGTPALT SRGLLEKDFQ.K .VAHFIHRGI
shmthc    GRAEKVLEAC SIACNKNTCP GD.RSALRPS GLRLGTPALT SRGLLEKDFQ.K .VAHFIHRGI
shmtsc    GRAEKVLEAC SIACNKNTCP GD.KSALRPS GLRLGTPALT SRGLLEEDFR.K .VAHFIHRGI

                              400             410
          1   123   123   1234       123  1       1    12   1234567890
shmtec    D.SIN...DE  ...AVI....E RIKG...KV.LDIC A.RYPV..YAH..........
shmtrc    ELTVQIQDDT GPRATLKEFKE KLAGD.EKHQRAVR ALRQEVESFAALFPLPGLPGF
shmthc    ELTLQIQSDT GVRATL.EFKE RLAGD..KYQAAVQ ALREEVESFASLFPLPGLPDF
shmtsc    ELTLQIQDAV GVKATLKEFME KLAGA.EEHQRAVT ALRAEVESFATLFPLPGLPGF
```

[a] Sequences highlighted for identity with rcSHMT.

same solution with successively increasing concentrations of heavy atom. Crystals were sensitive to most heavy atom compounds, but the following gave substituted derivatives that were useful for phasing: $K_3(UO_2)F_5$, Pt(ethylenediamine)Cl_2, 2-hydroxyethanethiolate(2,2′,2″-terpyridine)Pt(II)-nitrate, and $KAu(CN)_2$.

X-ray Diffraction Data Collection and Processing. Intensity data were collected at room temperature on an Raxis II image plate detector at a 95 mm crystal−detector distance with monochromatized CuKα radiation from a rotating anode source run at 80 kV and 100 mA. Anomalous pairs were collected for the uranyl derivative and used in the phasing.

Table 2: X-ray Diffraction Data, Phasing, and Model Refinement

	native	$K_3UO_2F_5$	$Pt(En_2)Cl_2$	$Pt(Pyr_4)$	$KAu(CN)_2$
		Data			
resolution	2.8	3.3	3.9	3.8	4.0
R_{merge}[a]	0.17[b]	0.27	0.24	0.24	0.24
$\langle I/\sigma(I)\rangle$ (overall/highest-resolution shell)	12.8/1.0	11.0/2.4	5.1/2.0	4.4/1.5	8.2/1.5
completeness	100.0	98.5	94.5	91.4	95.5
% reflections with multiplicity ≥ 5	94.3	49.8	44.5	31.7	55.6
Wilson plot *B*	80.5	103.7	132.3	89.8	107.4
		Phasing			
R_{deriv}[c]		0.14	0.11	0.13	0.13
R_{cullis}[d]		0.51	0.64	0.64	0.69
phasing power		1.81	1.04	1.04	1.09
mean figure of merit (centric/acentric)	0.44[e]	0.39/0.30	0.31/0.24	0.31/0.24	0.25/0.21
figure of merit after DM	0.73[f]				
		Refinement			
R_{work}	0.21				
R_{free}	0.28				
$\langle B\rangle$ (Å^2)	70.8				
no. of reflections	28454				
no. of free reflections	2885				
no. of atoms	7024				
torsional dynamics (no. of degrees of freedom)	3264				
rmsd for bond lengths (Å)	0.02				

[a] $R_{merge} = \Sigma\Sigma_i|I_h - I_{hi}|/\Sigma\Sigma_i I_h$, where I_h is the mean intensity of reflection *h*. [b] Statistics for the native crystal represent data merged over five separate crystals. [c] $R_{deriv} = \Sigma||F_{HP} - F_P|/\Sigma F_P$. [d] $R_{cullis} = \Sigma||F_{PH} - F_P| - |F_H(calc)||/|F_{PH} - F_P|$. [e] Figure of merit statistics for native data before DM represent aggregate statistics for both centric and acentric reflections to 3.5 Å. [f] Figure of merit statistics for native data after DM represent aggregate statistics for both centric and acentric reflections to 2.8 Å.

Oscillation data were integrated with Denzo (*24*) and merged with Scalepack (*24*) (Table 2).

Phase Calculation. A difference Patterson synthesis of the uranyl derivative was carried out to obtain heavy atom positions, and initial phases were calculated from the isomorphous and anomalous data for this derivative using PHASES (*25*). The other heavy atom derivatives did not yield readily interpretable difference Patterson maps. Heavy atom sites for these derivatives were found in difference Fourier syntheses using uranyl SIRAS phases and were validated by cross-difference Fouriers to the uranyl derivative. The expanded heavy atom site set was used to calculate MIRAS phases to 3.5 Å using isomorphous differences for all derivatives and anomalous differences for the uranyl derivative. Statistics from the phase calculation are summarized in Table 2.

Electron Density Maps. MIRAS phases were improved and extended to 3.0 Å resolution using the DM program from the CCP4 suite (*26*) with cyclic averaging about the noncrystallographic 2-fold axis coupled with histogram matching, solvent flattening, Sayre's equation, and multiresolution averaging. Electron density maps were calculated from these phases and interpreted using the program O (*27*). Initially, the model was fit as a polyalanine trace, and refined against the experimental phases followed by phase combination of the experimental and model phases using REFMAC (*28*). After several such cycles, the polypeptide could be traced throughout with the exception of parts of the amino and carboxyl terminal segments and of residues in the insert region around positions 244 and 245 (*E. coli* sequence numbering). Phases were then extended to 2.8 Å resolution and side chains added. The model was iteratively refined via torsion angle dynamics in XPLOR (version 3.843) with each refinement cycle followed by manual rebuilding in O. During iterative rebuilding, individual residue geometries were monitored with the program OOPs (*29*). Final refinement was carried out using CNS (version 0.5b) (*30*) to 2.8 Å resolution using a maximum likelihood target function (*31*, *32*) (Table 2). Of the 838 non-glycine residues in the final refined model, 44 lie outside of the allowed core regions of the Ramachandran plot and only nine of these were outside the relaxed allowed limits (Figure 1).

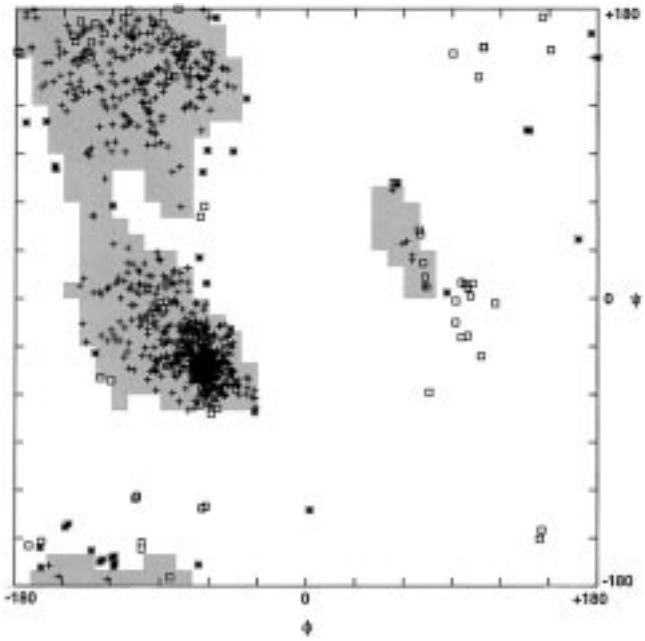

FIGURE 1: Ramachandran plot of the final refined model for rcSHMT.

In the final model, both molecules were missing the first 13 residues at the amino terminus. Molecule A was also missing six residues beginning at position 2446, and 26 side chains were partially or totally missing and were substituted with alanines. Molecule B was missing four residues beginning at position 2446 and had 31 residues with all or

FIGURE 2: Molscript (*59*) stereo backbone diagrams of the tight dimer of rcSHMT. Subunits are gray and white; the PLP group is shown as a space-filling representation and modeled 5-formyl-H_4PteGlu as a ball-and-stick representation.

part of their side chains absent and substituted with alanines. With few exceptions, these residues were polar, surface amino acids.

The electron density map of the isomorphous, unreduced rcSHMT crystals was calculated with amplitudes for data to 3.2 Å resolution from unreduced crystals and refined phases based on the reduced rcSHMT model without the PLP. The model for the unreduced form was subsequently refined in the same manner as the reduced form after manual adjustment of the PLP ring.

Hypothetical Model for the Complex of 5-Formyl-H_4PteGlu$_n$ with SHMT. Side chains missing from our refined model were inserted in O. Conformations for these missing side chains were set to the most commonly occurring rotamer from the database of Ponder and Richards (*33*). The structure for 5-formyl-H_4PteGlu was manually docked with the refined model of the reduced form of SHMT, positioning the Glu moiety in proximity to $K399_4$ to which it can be cross-linked and the N5−N10 conjugation site as close as possible to the substrate serine side chain in the putative external aldimine. After manual adjustment to optimize favorable interactions and relieve close contacts, the model for this complex was minimized with Discover version 2.98 (Molecular Simulations Inc., SanDiego, CA) using the cvff force field (*34*). Initially, 500 steps of steepest descent minimization were carried out in the absence of electrostatic terms followed by conjugate gradient minimization and the addition of electrostatic terms until the maximum Cartesian derivative of the energy was <0.01.

An electrostatic potential calculation (*35*) was carried out on the rcSHMT molecules from the minimized structure using the DELPHI module from the INSIGHT II suite (Molecular Simulations, Inc., San Diego, CA). The calculation was carried out with a protein monomer centered in a cubic box with a volume of 10^6 Å^3. The dielectric constant for the region inside the protein was set to 1.0, and the dielectric constant for the solvent surrounding the protein was set to 80. The calculated electrostatic potential map was used to identify charged regions on the molecular surface of each rcSHMT monomer.

The energy-minimized structure was also used to calculate interaction maps (*36*) for the graphical representation of noncovalent interactions between 5-formyl-H_4PteGlu and each of the monomers in the functional dimer using HINT (*37*) version 2.6I (Edusoft LC, Ashland, VA). These maps were calculated on a 1 Å grid over a volume defined by the interface between an rcSHMT monomer and the 5-formyl-H_4PteGlu. Separate interaction maps were calculated for polar and hydrophobic interactions between 5-formyl-H_4PteGlu and each rcSHMT monomer in the functional dimer. These maps were used to identify residues in the functional dimer which were involved in favorable polar or hydrophobic interactions with the 5-formyl-H_4PteGlu.

RESULTS

The crystal structure of rcSHMT closely resembles that described for hcSHMT (*22*). In the following description of rcSHMT, we make limited reference to the closely similar hcSHMT structure, but emphasize instead new information arising from this work, particularly that bearing on the mechanism of catalysis by SHMT.

Oligomeric Structure of rcSHMT. The crystal structure of rcSHMT consists of a tight dimer of identical monomers, which is the asymmetric unit, and these tight dimers are associated more loosely with another dimer asymmetric unit in forming a tetramer (Figure 2). The monomers of the tight dimer (subunits A_1B_1) have a contact surface of 8679 Å^3 across which multiple hydrogen-bonding, hydrophobic, and van der Waals contacts occur, including some residues present in the active site. The association between monomers in both the human and rabbit cytosolic tight dimers appears to be identical, thereby excluding any confounding effects of lattice interactions. As in other α-type PLP enzymes, amino terminal segments of about 40 amino acids extend away from each monomer and wrap around the other monomer of the tight dimer. The first 13 residues of the rcSHMT sequence, like the amino terminus of the hSHMT, are not visible in the electron density map. It seems unlikely that these residues could extend to make contacts with the other dimer, and thereby stabilize tetramer formation, but the amino terminus of A_1 in the A_1B_1 dimer is in proximity to the amino terminus of B_2 in the A_2B_2 dimer so that some interaction is possible. None of the 28 differences in sequence between rcSHMT and hcSHMT is likely to confer any signficant functional or structural differences on this pair of enzymes.

Interdimer contacts are almost entirely between corresponding subunits (A_1 with A_2 and B_1 with B_2) about the

Table 3: Environment of the PLP Group (Molecule A) in Different Intermediates of the SHMT Catalytic Reaction

PLP atom	amino acid	atom	unreduced (internal aldimine) (Å)	reduced (*gem*-diamine) (Å)
N1	D200	OD2	2.59	2.75
O3	K229	NZ	1.35	2.65
	H203	ND1	2.92	2.96
	S175	OG	4.32	3.16
PO1	S97	OG	2.56	2.47
PO2	S99	N	3.01	2.69
	S99	OG	2.99	2.85
	G263	N	2.82	2.63
PO3	Y55 (B)	OH	2.50	2.73

110 crystal lattice 2-fold axis. The imidazole side chains of His-134 stack on each other as is observed in the human enzyme. However, they also form hydrogen bonds with their tight dimer mate (Nϵ2 to Nϵ2), which implies different protonation states of these imidazole groups within a dimer. In addition to His-134, a strong ion pair immediately at the 2-fold axis between Arg-136 and Glu-167 links the two dimers. Asn-188 also makes a symmetric hydrogen bond contact with its corresponding mate, and close contacts between Met-169 and Phe-192 and between the Leu-191 side chain and the nonpolar part of the Lys-172 side chain contribute to stabilization of the tetramer.

Residues Forming Bonds to Pyridoxal Phosphate. As in other PLP enzymes, multiple ligands interact with the PLP group of reduced and internal aldimine rcSHMT (Table 3). The Asp-A200 side chain carboxylate stabilizes the positive charge of the PLP group at N1 (2.5 Å), but N1 also hydrogen bonds to the Asn-A102 amido side chain (2.8 Å). His-A126 is coplanar with the PLP group, as is the case for planar aromatic side chains at this position in other PLP enzymes.

Multiple hydrogen bonds anchor the phosphate group of the PLP of each subunit (those for subunit A listed here): Ser-A97, Ser-A99, His-A228, and Tyr-B55 and Gly-B263 of the other subunit of the dimer. The phosphate group of the rcSHMT PLP also lies at the amino terminal end of an α-helix (residues 98−110), as in other PLP enzymes. In contrast to AATase, but similar to ornithine decarboxylase (*38*) and dialkylglycine decarboxylase (*39*), there is no strong ion pair between the phosphate and a cationic amino acid side chain in this form of SHMT. The Arg-235 guanidino group is 4.1 Å from the PLP phosphate and is partially blocked by Tyr-55 from forming an ion pair interaction with the phosphate. This may explain the previous observation that unlike AATase, whose phosphate is a dianion over the pH range of the active enzyme, the phosphate of rcSHMT titrates between a monoanion and a dianion with a pK_a of 6.4 (*40*). Furthermore, the catalytically active enzyme can exist as a phosphate monoanion since the phosphate monomethyl ester of PLP, when reacted with apoenzyme, exhibits full catalytic activity (*41*). The observed pK_a suggests that the phosphate moiety in rcSHMT is in a hydrophilic pocket, and the structure exhibits multiple hydrogen-bonding groups around the phosphate. The lack of a positively charged Arg side chain within interaction distance of the phosphate is reflected in a pK_a that is only 0.3 pH unit higher than the solvent pK_a of the phosphate of PLP. It may also explain why PMP has a very low affinity for rcSHMT (K_d > 0.2 mM), whereas in AATase, PMP remains tightly bound (*42*).

The O3′ of the pyridoxal ring in reduced rcSHMT can hydrogen bond to the ϵ-amino group of Lys-229 and to the Oγ of Ser-175, and makes a long hydrogen bond to the Nδ1 of His-203. Some of these hydrogen bonds differ in length in the reduced and unreduced structures determined here and in the structure for the external aldimine modeled from them (Table 3). The PLP ring in the reduced aldimine form tilts by 15° counterclockwise about an axis through the C2 and C5 atoms (viewed from C2 to C5) of the PLP ring relative to its position in the internal aldimine structure (Figure 3) and also translates slightly. The phosphoryl group of the PLP does not move significantly. This change in conformation of the ring should be chemically identical to the change that takes place in formation of the *gem*-diamine structure with serine as the substrate. A model of the external aldimine with bound serine inferred from the reduced form of the *gem*-diamine shows that a further counterclockwise rotation of the PLP ring of 13° brings the serine amino group into near planarity with the PLP ring as required in the external aldimine (see below).

Residues Forming the Active Site. The active site at the PLP group is a cavity at the interface of the two monomers of the tight dimer, and it communicates with the solvent through two channels. The modeled position of serine substrate, which is occupied by a water molecule in the crystal structure, bound to the C4′ of the rotated PLP ring, brings its carboxylate group into proximity with Arg-363 and orients its hydroxymethyl side chain toward Glu-B57 and Tyr-B65 of the other monomer, as observed in hcSHMT (*22*) (Figure 3). The distance from the serine carboxylate, modeled in its *gem*-diamine configuration, to the guanidino side chain of Arg-363 is too long for formation of a strong ion pair interaction. Side chain dihedral angle changes in the arginine bring one of the guanidino NH groups within hydrogen bond distance of one of the carboxylate oxygens of the serine substrate (2.75 Å). The other NH is too far from the other carboxylate oxygen to form a hydrogen bond (~3.5 Å), but there is likely to be a strong electrostatic component of the interaction of these two groups. The side chains of Glu-B57 and Tyr-B65 are oriented toward the hydroxyl group of the putative bound substrate serine and are candidates for the base which abstracts the proton from this side chain (see the Discussion). These two enzyme side chains form no hydrogen bonds to other groups in the structure.

Analysis of the charge distribution of the SHMT structure shows a clearly recognizable surface of strong positive charge surrounding a channel extending out of the active site, which is the likely binding site of the polyglutamate tail of the folate group (Figure 5a). Within this site is the $Lys399_4$ to which carbodiimide-activated 5-formyl-H_4PteGlu and 5-formyl-H_4-$PteGlu_5$ are cross-linked (*43*).

DISCUSSION

Mechanistic Implications of the Structure of rcSHMT. A principal objective of this structure determination is to identify the functional groups of SHMT that participate in the steps of the reaction which have been characterized through solution studies of the mechanism (*3*). Although a complete set of structures for the intermediates of the SHMT reaction pathway is not yet available, the considerable

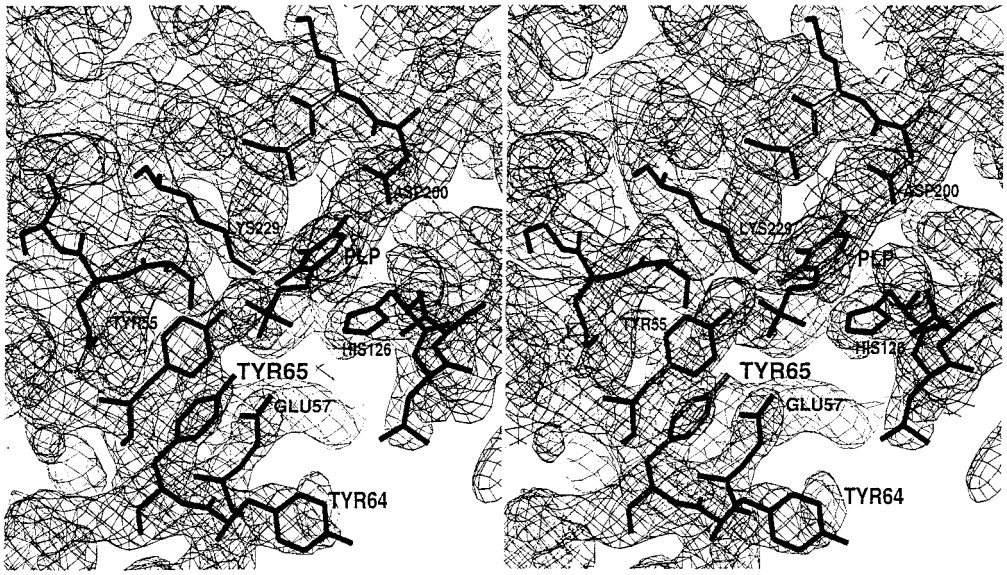

FIGURE 3: Stereo figure of the electron density around the PLP group of rcSHMT.

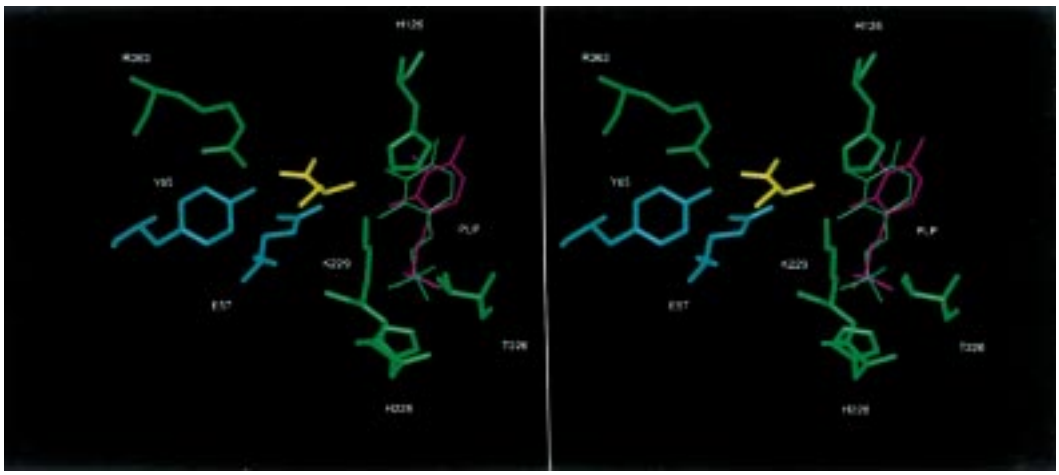

FIGURE 4: Stereoview of the active site region of rcSHMT with the modeled serine substrate (yellow) and the PLP group shown in its internal aldimine (magenta) and *gem*-diamine (green) positions.

amount of data from mechanistic and site mutant studies in solution and the similarities of SHMT to other α-type PLP enzymes provide a basis for inferences about the structures of intermediates along the reaction pathway. The crystal structures of the internal aldimine and reduced internal aldimine, with the obligatory chemical structures of the substrate-bound intermediates, are chemically equivalent to the holoenzyme and the first intermediate, the *gem*-diamine, in the serine cleavage reaction. These structures define the position of the substrate amino group linked to C4′ of the PLP ring and of the carboxyl group ion-paired to Arg-363, and greatly restrict the position and orientation of the amino acid substrate. Solution studies of nonspecific substrates such as *β*-phenylserine, allothreonine, and L- and D-alanine also impose criteria of consistency on the definition of the orientation of the C3 hydroxyl group of the substrate binding site. Finally, solution studies, mechanistic considerations, and the modeled structures of the amino acid complexes with SHMT support a single mode of binding for the folate cofactor. We describe here a mechanism-based interpretation of the structure of rcSHMT derived from these data and assumptions, which offers testable hypotheses.

Modeling the gem-Diamine Intermediate. The first step in the catalytic reaction cycle is the formation of the *gem*-diamine intermediate shown as structure II in Scheme 1. In a previous study on substrate amino acid binding, no evidence could be found for a stable noncovalently bound amino acid prior to formation of the *gem*-diamine intermediate (*44*). We have used the above constraints on serine substrate binding with the structures of the internal aldimine and the reduced aldimine, this latter being stereoelectronically equivalent to the *gem*-diamine intermediate, to model the *gem*-diamine intermediate.

In forming the *gem*-diamine intermediate, C4′ of PLP goes from an sp^2 hybrid to an sp^3 hybrid like that observed here in the reduced aldimine linkage of PLP to Lys-229. In AATase, this change in hybridization induces a rotation primarily around the C5−C5′ bond of PLP of about 20° (*8*). This places the *ϵ*-amino group of Lys-259 in AATase out of the plane of the pyridine ring and on the *si* face of the original internal aldimine. The structure of reduced rcSHMT shows that reduction of the internal aldimine with $NaCNBH_3$ results in a change in the PLP ring position at the active site similar to that found in the *gem*-diamine in AATase. In reduction

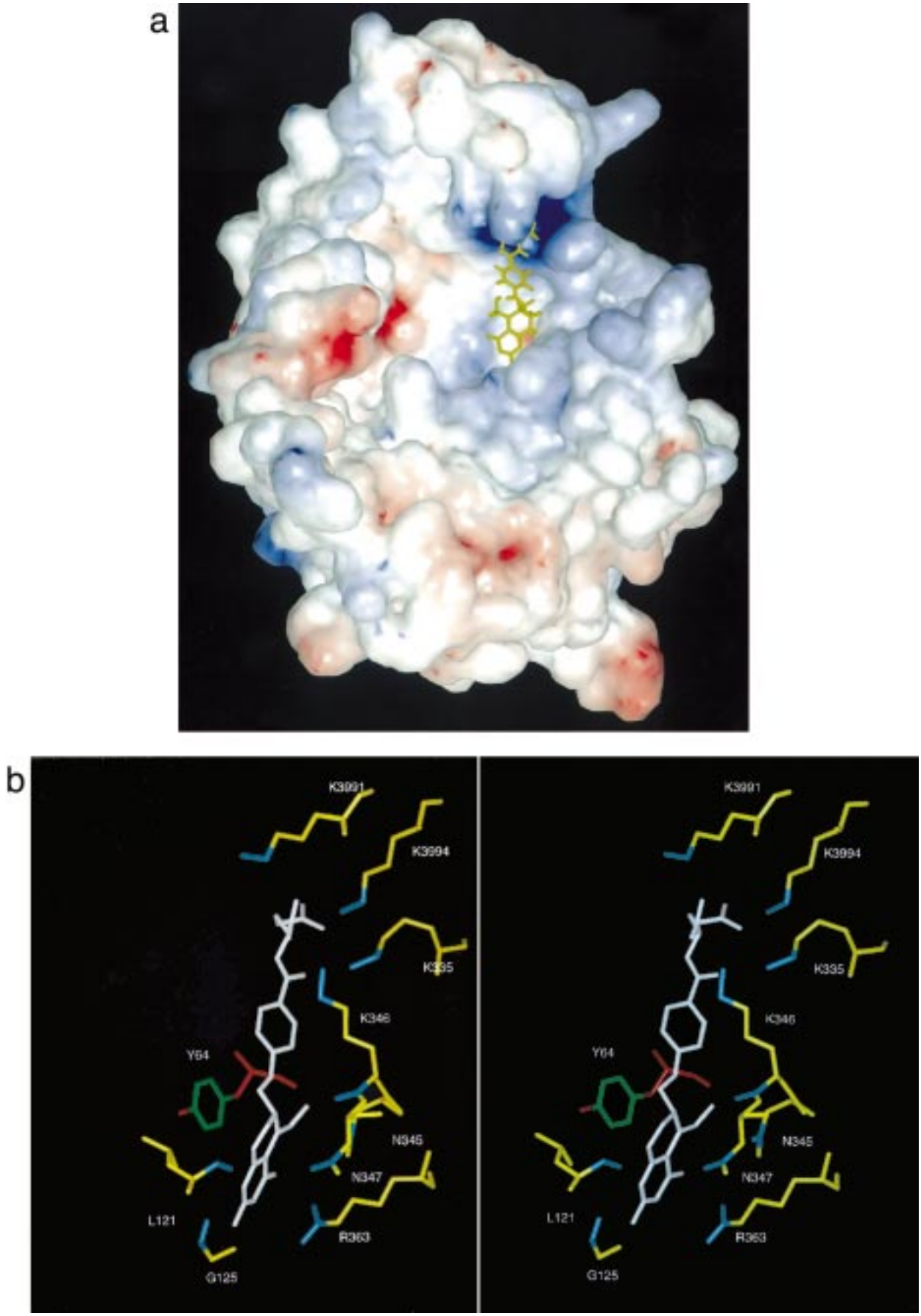

FIGURE 5: (a) Surface electrostatic potential map of rcSHMT. Positive integrated charge is shown as blue and negative as red. The 5-formyl-H_4PteGlu is shown in yellow. (b) Stereoview of the modeled structure of the bound $H_4PteGlu_n$ at the active site of rcSHMT showing groups which interact with it. Molecule A is yellow and molecule B red; groups making polar interactions (including hydrogen bonds) are cyan and those making hydrophobic interactions green.

of rcSHMT by $NaCNBH_3$, a hydride ion, rather than a substrate amino group, makes a nucleophilic attack on the *re* face of C4′. We find in the reduced rcSHMT that the pyridine ring has rotated relative to its orientation in the internal aldimine by 15° about an axis approximately through the C2 and C5 atoms of the ring in the counterclockwise direction viewed toward C5. Replacing the attacking hydride ion by the serine amino group and locating its carboxylate near Arg-363 permit orientation of the amino acid substrate corresponding to the *gem*-diamine intermediate. The Nϵ-amino group of Lys-229 lies on the *si* face side of the PLP ring, and the angle defining the nonplanarity of the Nϵ of the lysine side chain with the PLP ring (C4−C4A−Nϵ) is 137° in the reduced form and 171° in the unreduced form of the internal aldimine in our rcSHMT structures.

In contrast to AATase, the amino acid substrates of SHMT bind at the active site in the anionic form with an unprotonated α-amino group (*44*). In AATase, the amino acid substrate binds with a protonated amino group and must transfer this proton to an active site residue prior to nucleophilic attack at C4′. This proton acceptor in AATase is the unprotonated nitrogen of the ϵ-amino group of Lys-257 of the internal aldimine (*45*). However, in cSHMT this nitrogen of the internal aldimine is protonated at all pH values over which the enzyme is active, consistent with the absence of a proton transfer from the substrate amino group on formation of the Michaelis complex.

In AATase, the substrate α-carboxylate group forms an ion pair with Arg-386 in the active site that is coupled to formation of the closed form of the enzyme. In rcSHMT, Arg-363 can form an ionic interaction with the substrate serine carboxylate group positioned to form the *gem*-diamine, if changes in only the side chain dihedral angles of Arg-363 are introduced. In this modified conformation of Arg-363, one hydrogen bond (2.75 Å) from the guanidino NH to a carboxylate oxygen can form, but the other potential hydrogen bonding pair is too long for a hydrogen bond. In addition, the Ser-35 side chain hydroxyl group can hydrogen bond to the modeled substrate carboxyl group as well as to the Arg-363 guanidino side chain. These two interactions have consequences for identifying and defining the "open" and "closed" forms of SHMT (see below).

Conversion of the gem-Diamine to the External Aldimine (III to IV, Scheme 1). The nucleophilic attack of the substrate amino group on the internal aldimine results in the *gem*-diamine intermediate with a protonated nitrogen on the substrate and an unprotonated ϵ-amino nitrogen on Lys-229. Expulsion of the Lys-229 amino group from the *gem*-diamine intermediate requires two additional steps: a formal proton transfer from the substrate amino group to the Lys amino group and a further rotation of the PLP ring relative to the Lys-229 Nϵ-amino group to bring the Lys-229 Nϵ−C4′ aldimine bond perpendicular to the plane of the PLP ring (II to III, Scheme 1).

Shafer has suggested from studies with D-serine dehydratase that this proton transfer and rotation of the PLP ring in forming the protonated Lys-229 Nϵ-amino group perpendicular to the ring is important for determining substrate specificity in PLP enzymes (*46*). We have described here the movement of the PLP ring on reduction of the internal aldimine linkage, which is equivalent to that which occurs in forming the first *gem*-diamine intermediate. A further rotation of the PLP ring by 13° about the C2−C5 axis of the PLP is sufficient to attain the stereochemistry of the external aldimine with the substrate amino group in the plane of the PLP ring.

Mutation of Thr-226 to Ala in *E. coli* SHMT results in the accumulation of the *gem*-diamine complex absorbing at 343 nm with a small fraction of the PLP as the external aldimine absorbing at 425 nm. The conversion of the amino acid substrates and substrate analogues to the external aldimine is a slow, rate-determining step (*40*). Thr-226 is conserved as either a Thr or Ser in all known SHMTs, and in modeling the active site of *E. coli* SHMT, Pascarella et al. (*21*) remarked that in the external aldimine the released Lys-229 ϵ-amino group could hydrogen bond to Oγ of Thr-226. Our structure confirms that rotations at χ_3 and χ_4 of the expelled Lys-229 side chain bring the ϵ-amino group within hydrogen bonding distance of Thr-226. This interaction between Thr-226 and the Lys-229 Nϵ-amino group should favor formation of the external aldimine by stabilizing the unbonded Lys-229 through formation of the hydrogen bond to the Thr-226 side chain, which is sequestered from solvent and has no other candidate groups to which its side chain can hydrogen bond. The inability to form this hydrogen bond in the T226A mutant is consistent with expulsion of Nϵ from the *gem*-diamine becoming very slow, resulting in the accumulation of the *gem*-diamine intermediate absorbing at 343 nm.

The role of Thr 226 as a hydrogen bond partner to unprotonated Lys-229 may also contribute to substrate specificity of SHMT. In the external aldimine, formation of this hydrogen bond will maintain the free Lys-229 Nϵ-amino group in its unprotonated form necessary for a nucleophilic attack on C4′ after exchange of the electrophilic groups at Cα of glycine (IV, Scheme 1). In the external aldimine, the 2*R* proton of the L-amino acid substrate is nearly perpendicular to the original *si* face of C4′ of PLP (IV, Scheme 1). In transaminases, the Nϵ-amino group of the active site lysine acts as a base to accept this 2*R* proton, resulting in the formation of the quinonoid intermediate (structure V, Scheme 1). The protonated Nϵ of Lys-229 then donates the proton back to C4′ of PLP to convert the quinonoid into the ketimine intermediate as observed with AATase (V to VI, Scheme 1). To prevent abortive transamination, SHMT must block transfer of the 2-*pro-R* proton of the external aldimine to the Lys-229 ϵ-amino group, and we suggest that this is effected by hydrogen bond formation between the Thr-226 side chain hydroxyl and the Nϵ of Lys-229.

In SHMT, a slow transamination occurs with the nonspecific L- and D-alanine substrates (*47*), but not with L-serine. Furthermore, the slow rate of racemization of L- and D-alanine relative to quinonoid intermediate formation indicates that the bases in SHMT accepting the Cα proton of these two isomers are different (*47*). The rate of transamination of L-alanine is increased 5-fold in the T226A mutant, consistent with a role for this threonine in suppressing protonation of the Lys-229 ϵ-amino group in this reaction. In contrast, the transamination rate of D-Ala in the T226A mutant is not affected, supporting a role for a base distinct from Lys-229. The most likely candidate for this base is the carboxylate side chain of Glu-B57 or a water molecule activated by this group.

Thr-226 in SHMT is also present as a conserved Ser-255 in AATases (*6*). To our knowledge, this residue has not been changed by site-directed mutagenesis in probing its function. It is a ligand of the PLP phosphate group in both the open and closed conformations, but as in SHMT, small side chain rotations about χ_3 and χ_4 of the Lys-258 side chain could lead to formation of a hydrogen bond to the Ser-255 side chain hydroxyl. We note that Tyr-A225 and Tyr-B70 could also hydrogen bond to Lys-255 through their phenolic OH groups in AATase.

Retroaldol Cleavage of 3-Hydroxy Amino Acids. From the structure of hcSHMT, it was suggested that the side chains of Glu-B57 and Tyr-B65 of the opposite monomer of the tight dimer are candidates for the base which abstracts the proton from the substrate serine side chain hydroxyl group in the retroaldol cleavage reaction. This is confirmed in the rcSHMT structure and in the model of the *gem*-diamine intermediate based on the structure of the aldimine-reduced rcSHMT. Using the constraints imposed by the required positions of the substrate serine amino group as a substituent of the tetrahedral C4′ carbon and the serine carboxylate paired with the guanidino group of the Arg 363 side chain, we can also explain the observations that both L-allothreonine (the hydroxyl group on C3 and amino group on C2 are *erythro*) and *erythro* β-phenylserine are better substrates by 1 order of magnitude than their corresponding *threo* isomers (*48*, *49*). Superposition of *erythro* β-phenylserine and allothreonine at the active site, subject to the above constraints, directs the β-phenyl group and the methyl group side chains to a cavity adjacent to the PLP group, which is defined by residues Tyr-B55, Gly-B262, Gly-B263, Leu-A127, His-A126, and Phe-B257. The side chain of Glu-57 from the other monomer of the tight dimer is poised adjacent to the β-hydroxyl group and is a good candidate for the basic residue which abstracts the proton in the retroaldol cleavage reaction; in contrast, substrate threonine in the same site is oriented with its 3-OH away from Glu-57. The efficiency of β-phenylserine as a substrate of SHMT is likely due to orientation of the 3-hydroxyl group toward Glu-57 and to the binding of the phenyl ring in this cavity, and possibly also to elevation of the p*K* of the Glu-57 side chain carboxylate through the introduction of the phenyl ring to this site. Binding of these hydrophobic side chains would probably not be favorable if the phosphate group of the PLP were in its dianionic form.

Quinonoid Formation and Hydroxymethyl Transfer to $H_4PteGlu_n$. We have previously inferred from physical properties and by analogy to AATase that SHMT undergoes an open to closed conformational change upon binding of substrates with a 3-hydroxyl group. The crystal structures of human and rabbit cytosolic SHMT have been assumed to be in the open conformation, since no ligands are present. We note that SHMT lacks any obvious hinge region residues or kink in the long α-helix connecting the large and small domains, like Gly-326 and Gly-38 of AATase, at which domain movements are likely to be levered. Furthermore, as described above, the inferred position of bound serine substrate in the rcSHMT structure requires only a change in conformation of the Arg-363 side chain in forming an ion pair interaction with one good hydrogen bond to the substrate serine carboxylate group. Finally, Gly-38 in AATase, which forms a hydrogen bond with the carboxylate of the Asp substrate only on formation of the closed form, corresponds to Ser-35 in rcSHMT, which can hydrogen bond to the carboxylate of the serine substrate in the unreduced structure described here. Thus, either the form we have crystallized is the closed form resembling the closed form of AATase, or the operational definition of open and closed forms of SHMT does not describe conformational states such as those of AATase. We favor the latter hypothesis in which the closed form of SHMT, defined by its increased stability to thermal denaturation and diminished level of exchange of protons with solvent, is not a major change in enzyme conformation or relative domain position, but rather reflects the formation of new hydrogen bonds and an ion pair between bound serine substrate and enzyme functional groups which are not hydrogen bonded in the open form of the enzyme in the absence of bound substrate. Specifically, ion pair and hydrogen bond interactions between the serine substrate carboxylate group and the guanidino side chain group of Arg-363, hydrogen bond formation of Glu-57 with the side chain hydroxyl group of the serine, and the covalent linkage of the α-amino group in forming the external aldimine with attendant changes in the PLP ring orientation may constitute the changes in structure which define the more stable closed conformation of SHMT. Others have concluded that several members of the α-group of PLP enzymes do not have the several angstrom displacement of the small and large domains seen in AATase upon binding substrates (*50*). In the absence of evidence to the contrary, we make the assumption that there are no large changes in the SHMT polypeptide conformation during the catalytic reaction.

On this assumption, the modeled structure of the external aldimine greatly restricts the possible binding site for the $H_4PteGlu_n$ cofactor to which the cleaved hydroxymethyl group is transferred on cleavage from serine. The pteridine ring of the folate can be oriented in only one orientation adjacent to the bound serine substrate, and previous studies have shown that a carboxyl group of the inhibitor 5-formyl-$H_4PteGlu_n$ can be cross-linked to Lys-399_4 in rcSHMT (*43*), thereby defining the direction of the polyglutamate moiety of the folate. With these constraints, we have modeled, with energy-minimized coordinate refinement, the structure of the complex of 5-formyl-H_4PteGlu bound to the putative external aldimine structure and correlated it with existing data to draw testable conclusions.

The model directs the distal γ-glutamyl residues of the folate to a cationic surface region of the protein largely in the C-terminal domain of the same monomer to which the pteridine ring binds (Figure 4b). This cationic surface includes Lys-A346, Lys-A335, Arg-A358, Lys-A146, Arg-A324, Lys-A308, and Arg-A412, residues which are completely conserved in human, rabbit, and sheep SHMTs (Table 1). Phenylglyoxal modification studies on sheep SHMT implicated Arg-242 and Arg-412 in H_4PteGlu binding (*51*). Arg-412 lies in the putative polyglutamate binding site inferred from the structure of rcSHMT, but is more likely to interact with γ-glutamyl residues more distal than the first residue. Arg-242 from the other subunit of the tight dimer is at the base of the partially disordered insertion segment common to the eukaryotic SHMTs, but absent in the *E. coli* enzyme. While it is too far removed to interact with H_4-PteGlu as modeled, the flexibility of this insertion segment, which lies on one side of the polyglutamate binding channel

and may form a top of this channel, could affect access of this cofactor to the active site. The fact that this flexible insertion loop occurs in eukaryotes, but is absent in *E. coli*, may point to functional distinctions in polyglutamate binding between *E. coli* and eukaryotes. It is known that the distal carboxyl groups of $H_4PteGlu_n$ in *E. coli* are α-linked in contrast to the γ-linked residues in eukaryotes (*52*).

The pteridine ring of $H_4PteGlu_n$ lies between the two monomers of the tight dimer and makes a number of contacts with the protein: exocyclic N2 can hydrogen bond to the carbonyl oxygen of Gly-A125; exocyclic O_4 makes a short hydrogen bond to the phenolic hydroxyl group of Tyr-A65; cyclic N8 can hydrogen bond to Asn-A347; and side chains of Leu-A121 and Leu-A127 line one side of the pocket. The phenyl group of the *p*-aminobenzoyl group may stack on the side chain of Tyr-B64 with modest rotations of either or both phenyl rings, and the formyl group on N5 of the folate inhibitor could hydrogen bond to Asn-A345 and the carbonyl of K-346. Asn-345 is also hydrogen bonded to the Arg-363 guanidino group that forms an ion pair with the carboxylate of the serine substrate. These two interactions of the formyl group may be responsible for the tight binding of the SHMT inhibitor 5-formyl-H_4PteGlu and also for the observation that only one rotamer of the formyl group, which exists most likely as the enolate conjugated to N5 of $H_4PteGlu_n$, binds to SHMT (*53*). The rotamer in which the hydroxymethyl group is facing O4 of the pteridine ring cannot be accommodated in the binding site as we have modeled it with bound 5-formyl-$H_4PteGlu_n$. The other rotamer can fit and will make a hydrogen bond with the rotated side chain of Asn-A345.

A further test of our model of the binding of serine and $H_4PteGlu_n$ is that it must conform to the stereochemical constraints for the transfer of the hydroxymethyl group from (3*R*)-[3-^{3}H]serine to form (11*R*0)-[11-^{3}H]CH_2-$H_4PteGlu_n$ (*54*, *55*). This requires a direct nucleophilic attack of the N5 of H_4PteGlu on the *re* face of the free formaldehyde to generate 5-hydroxymethyl-$H_4PteGlu_n$. This requirement is not met in our modeled ternary complex of serine and $H_4PteGlu_n$. In our model, the pteridine ring is maximally inserted into the active site cavity, but is still too far displaced (about 8 Å) from the active site to directly accept the serine C3 hydroxyl group at its N5 and N10 positions. However, the phenolic group of Tyr-B65, which interposes between the hydroxymethyl group of the serine and the N5−N10 positions of the H_4PteGlu, could form a hemiacetal with the formyl group produced by deprotonation of the serine side chain hydroxyl group by Glu-57 and breaking of the Cα−C*β* bond. Furthermore, the short hydrogen bond between the Tyr-B65 hydroxyl group and the exocyclic O_4 of the pteridine ring could activate the Tyr-B65 hydroxyl group for formation of such a hemiacetal. Transfer of the hydroxymethyl group to theTyr-B65 side chain would place the hemiacetal group about 5.2 Å from the N5 of the folate to which it could be transferred, possibly with some local changes in side chain conformation. In this hypothetical mechanism, Tyr-B65 would serve as the shuttle of the hydroxymethyl group between the external aldimine-bound serine substrate and the folate cofactor. We cannot rule out the possibility that the Tyr-B65 phenolate ion could make a direct SN_2 displacement of the C_α bond of IV forming a hemiacetal directly. One attractive feature of the hemiacetal intermediate hypothesis is that it would explain why the rapid cleavage of serine in the absence of $H_4PteGlu_n$ results in the very slow release of formaldehyde (*56*, *57*). We have postulated that the formaldehyde forms a complex with a group at the active site (*58*), and Tyr-B65 is a candidate for that group. If this hypothesis is true, then the Y65F mutant of rcSHMT should cleave serine and rapidly release formaldehyde. This would implicate Tyr-B65 in formation of the hemiacetal intermediate and could explain why in our model N5 of $H_4PteGlu$ is not close to C3 of serine in the external aldimine.

REFERENCES

1. Schirch, L. (1982) *Adv. Enzymol. Relat. Areas Mol. Biol. 53*, 83−112.
2. Bairoch, A., and Boeckmann, B. (1991) *Nucleic Acids Res. 19*, 2247−2249.
3. Schirch, V. (1998) in *Comprehensive Biological Catalysis* (Sinnott, M., Ed.) Vol. 1, pp 211−252, Academic Press, San Diego, CA.
4. Smith, D. M., Thomas, N. R., and Gani, D. (1991) *Experientia 47*, 1104−1118.
5. Schirch, V., Shostak, K., Zamora, M., and Gautam-Basak, M. (1991) *J. Biol. Chem. 266*, 759−764.
6. Alexander, F. W., Sandmeier, E., Mehta, P. K., and Christen, P. (1994) *Eur. J. Biochem. 219*, 953−960.
7. Mehta, P. K., Hale, T. I., and Christen, P. (1993) *Eur. J. Biochem. 214*, 549−561.
8. Kirsch, J. F., Eichele, G., Ford, G. C., Vincent, M. G., and Jansonius, J. N. (1984) *J. Mol. Biol. 174*, 497−525.
9. McPhalen, C. A., Vincent, M. G., and Jansonius, J. N. (1992) *J. Mol. Biol. 225*, 495−517.
10. Okamoto, A., Higuchi, T., Hirotsu, K., Kuramitsu, S., and Kagamiyama, H. (1994) *J. Biochem. 116*, 95−107.
11. Henning, M., Grim, B., Contestabile, R., John, R. A., and Jansonius, J. N. (1997) *Proc. Natl. Acad. Sci. U.S.A. 94*, 4866−4871.
12. Momany, C., Ernst, S., Ghosh, R., Chang, N. L., and Hackert, M. L. (1995) *J. Mol. Biol. 252*, 643−655.
13. Momany, C., Ghosh, R., and Hackert, M. L. (1995) *Protein Sci. 4*, 849−854.
14. Shen, B. W., Ramesh, V., Müller, R., Hohenester, E., Hennig, M., and Jansonius, J. N. (1994) *J. Mol. Biol. 243*, 128−130.
15. Toney, M. D., Hohenester, E., Keller, J. W., and Jansonius, J. N. (1995) *J. Mol. Biol. 245*, 151−179.
16. Watanabe, N., Sakabe, N., Sakabe, K., Higashi, T., Sasaki, K., Aibara, S., Morita, Y., Yonoha, K., Toyama, S., and Fukutani, H. (1989) *J. Biochem. 105*, 1−3.
17. Antson, A. A., Demidkina, T. V., Gollnick, P., Dauter, Z., Von Tersch, R. L., Long, J., Berezhnoy, S. N., Phillips, R. S., Harutyunyan, E. H., and Wilson, K. S. (1993) *Biochemistry 32*, 4195−4206.
18. Stover, P., Kruschwitz, H., Schirch, V., and Wright, H. T. (1993) *J. Mol. Biol. 230*, 1094−1096.
19. Kazanina, G., Radaev, S., Wright, H. T., and Schirch, V. (1998) *J. Struct. Biol. 123*, 169−174.
20. Renwick, S. B., Skelly, J. V., Chave, K. J., Sanders, P. G., Snell, K., and Baumann, U. (1998) *Acta Crystallogr. D54*, 1030−1031.
21. Pascarella, S., Angelaccio, S., Contestabile, R., Delle Fratte, S., Di Salvo, M., and Bossa, F. (1998) *Protein Sci. 7*, 1976−1982.
22. Renwick, S. B., Snell, K., and Baumann, U. (1998) *Structure 6*, 1105−1116.
23. di Salvo, M., Delle Fratte, S., De Biase, D., Bossa, F., and Schirch, V. (1998) *Protein Expression Purif. 13*, 177−183.
24. Otwinowski, W., and Minor, W. (1997) *Methods Enzymol. 276*, 307−326.
25. Furey, W., and Swaminathan, S. (1997) *Methods Enzymol. 277*, 590−620.
26. Collaborative Computational Project, number 4 (1994) *Acta Crystallogr. D50*, 760−763.
27. Jones, T. A., Zou, J. Y., Cowan, S. W., and Kjeldgaard, M. (1991) *Acta Crystallogr. A47*, 110−119.

28. Murshudov, G. N., Vagin, A. A., and Dodson, E. J. (1997) *Acta Crystallogr. D53*, 240−245.
29. Kleywegt, G. J., and Jones, T. A. (1996) *Acta Crystallogr. D52*, 829−832.
30. Brunger, A. T., Adams, P. R., Clore, G. M., Gros, P., Grosse-Kunstleve, R. W., Jiang, J. S., Kuszewski, J., Nilges, M., Pannu, N. S., Reid, R. J., Rice, L. M., Simonson, J., and Warren, G. (1998) *Acta Crystallogr. D54*, 905−928.
31. Pannu, N. S., and Read, R. J. (1996) *Acta Crystallogr. A52*, 654−668.
32. Adams, P. D., Pannu, N. S., Read, R. J., and Brunger, A. T. (1997) *Proc. Natl. Acad. Sci. U.S.A. 94*, 5018−5028.
33. Ponder, J. W., and Richards, F. M. (1987) *J. Mol. Biol. 193*, 775−791.
34. Dauber-Osguthorpe, P., Roberts, V. A., Osguthorpe, D. J., Wolffe, J., Genest, M., and Hagler, A. J. (1988) *Proteins: Struct., Funct., Genet. 4*, 31−47.
35. Gislon, M., Sharp, K., and Honig, B. (1988) *J. Comput. Chem. 9*, 327.
36. Abraham, D. J., Kellogg, G. E., Holt, J. M., and Ackers, G. K. (1997) *J. Mol. Biol. 272*, 613−632.
37. Wireko, F. C., Kellogg, G. E., and Abraham, D. J. (1991) *J. Med. Chem. 34*, 758−767.
38. Momany, C., Ernst, S., Ghosh, R., Chang, N.-L., and Hackert, M. L. (1995) *J. Mol. Biol. 252*, 643−655.
39. Toney, M. D., Hohenester, E., Keller, J. W., and Jansonius, J. N. (1995) *J. Mol. Biol. 245*, 151−179.
40. Quashnock, J. M., Chlebowski, J. F., Martinez-Carrion, M., and Schirch, L. (1983) *J. Biol. Chem. 258*, 503−507.
41. Schirch, L., and Schnackerz, K. D. (1978) *Biochem. Biophys. Res. Commun. 85*, 99−106.
42. Martinez-Carrion, M. (1975) *Eur. J. Biochem. 54*, 39−43.
43. Huang, T., Wang, C., Maras, B., Barra, D., and Schirch, V. (1998) *Biochemistry 37*, 13536−13542.
44. Angelaccio, S., Pascarella, S., Fattori, E., Bossa, F., Strong, W., and Schirch, V. (1992) *Biochemistry 31*, 155−162.
45. Kirsch, J. F., Eichele, G., Ford, G. C., Vincent, M. G., and Jansonius, J. N. (1984) *J. Mol. Biol. 174*, 497−525.
46. Federiuk, C. S., and Shafer, J. A. (1983) *J. Biol Chem. 258*, 5372−5378.
47. Shostak, K., and Schirch, V. (1988) *Biochemistry 27*, 8007−8014.
48. Schirch, L., and Gross, T. (1968) *J. Biol. Chem. 243*, 5651−5655.
49. Ulevitch, R. J., and Kallen, R. G. (1977) *Biochemistry 16*, 5342−5350.
50. Shen, B. W., Hennig, M., Hohenester, E., Jansonius, J. N., and Schirmer, T. (1998) *J. Mol. Biol. 277*, 81−102.
51. Usha, R., Savithri, H. S., and Rao, N. A. (1992) *J. Biol. Chem. 267*, 9289−9293.
52. Ferone, R., and Roland, S. (1980) *Proc. Natl. Acad. Sci. U.S.A. 77*, 5802−5806.
53. Stover, P., and Schirch, V. (1992) *Biochemistry 31*, 2155−2164.
54. Matthews, R. G., and Drummond, J. T. (1990) *Chem. Rev. 90*, 1275−1290.
55. Vanoni, M. A., Lee, S., Floss, H. G., and Matthews, R. G. (1990) *J. Am. Chem. Soc. 112*, 3987−3993.
56. Chen, M. S., and Schirch, L. (1973) *J. Biol. Chem. 248*, 3631−3635.
57. Webb, H. K., and Matthews, R. G. (1995) *J. Biol. Chem. 270*, 17204−17209.
58. Kraulis, P. (1991) *J. Appl. Crystallogr. 24*, 946−950.

BI9904151